Discrete Curvature Flow for Hyperbolic 3-Manifolds with Complete Geodesic Boundaries

Xiaotian Yin [1], Miao Jin [1], Feng Luo [2] and Xianfeng Gu [1]

[1]Center for Visual Computing
Stony Brook University
Stony Brook, NY 11794, U.S.A
{xyin, mjin, gu}@cs.sunysb.edu

[2]Department of Mathematics
Rutgers University
Piscataway, NJ 08854, U.S.A
fluo@math.rutgers.edu

June 26, 2008

Abstract

Every surface in the three dimensional Euclidean space have a canonical Riemannian metric, which induces constant Gaussian curvature and is conformal to the original metric. Discrete curvature flow is a feasible way to compute such canonical metrics. Similarly, three dimensional manifolds also admit canonical metrics, which induce constant sectional curvature. Canonical metrics on 3-manifolds are valuable for the study of 3D topology and have the potential for volumetric parameterization and shape matching.

This paper generalizes discrete curvature flow from surfaces to hyperbolic 3-manifolds with complete geodesic boundaries. The metric deforms according to the curvature, until the curvature is constant everywhere. The theoretical results are introduced, the algorithm is explained in details, and thorough experiments are carried out to demonstrate the effectiveness and efficiency of discrete 3-manifold curvature flow.

Contents

1 Introduction

Studying the topological and geometric structures of three dimensional manifolds has fundamental importance in science and engineering. Computational algorithms for 3-manifolds can help topologists and geometers to investigate the complicated structures of 3-manifolds, they also have great potential for wide applications in the engineering world. The most direct applications include volumetric parameterizations, volumetric shape analysis, volumetric deformation, solid modeling and etc.

Figure 2 shows a simple example for volumetric parameterization for the volumetric Max Planck model. The topology of the volume is very simple, a topological ball. A 3-manifold with more complicated topology is shown in figure 3. In general, topology of 3-manifolds is extremely difficult to analyze. The perception of the topological structures of 3-manifolds are in general beyond human's intuition, because most 3-manifolds can not be realized in $\mathbb{R}^3$. A natural approach to study 3-manifold is to map the 3-manifold onto the three dimensional space, so that human beings can interpret them with concrete tangible experiences. It is of great value for the advancement of science.

This is equivalent to construct a parameterization for an abstract 3-manifold by a domain in $\mathbb{R}^3$. We can make a natural analogy using the surface parameterization. Most surfaces can not be realized isometrically in the plane $\mathbb{R}^2$. Figure 1 shows one example. A surface with negative Euler number is parameterized and is conformally mapped to the hyperbolic space $\mathbb{H}^2$. The three boundaries

	Surface	3-Manifold
Manifold	with negative Euler number with boundaries Fig.1	Hyperbolic 3-manifold with geodesic boundaries Fig.3
Building Block	hyperbolic right-angled hexagons Fig.1	Truncated hyperbolic tetrahedra Fig.7
Curvature	Gaussian curvature Fig 8	Sectional curvature Fig.8, Fig.9
Algorithm	Discrete Ricci flow	Discrete curvature flow
Parameter domain	Upper half plane $\mathbb{H}^2$ Fig.1	Upper half space $\mathbb{H}^3$ Fig.18

Table 1: Correspondence between surface and 3-manifold parameterizations.

are mapped to geodesics. Given two arbitrary boundaries, there exists a unique geodesic orthogonal to both boundaries. Three such geodesics partition the whole surface into two right-angled hexagons as shown in (c). The surface is mapped periodically to $\mathbb{H}^2$, frame (c) shows one period, frame (d) shows the periodic embedding.

This work focuses on generalizing the parameterizations of open surfaces with negative Euler numbers to hyperbolic 3-manifolds with boundaries as shown in Fig. 3, where the 3-manifold is the 3-ball with a knotted pipe removed. There are many intrinsic similarities and some fundamental differences. We summarize the corresponding concepts for surfaces and 3-manifolds respectively in table 1: the building blocks for surfaces are right-angled hyperbolic hexagons as shown in figure Fig.1 frame (c); for 3-manifolds are truncated hyperbolic tetrahedra shown in Fig.7. Both cases require to perform curvature flows. The curvature used in the surface case is the vertex curvature in Fig.8, that in 3-manifold case is the edge curvature in Fig. 9. The parameter domain for the surface case is the hyperbolic space $\mathbb{H}^2$ using the upper half plane model; the domain for 3-manifold case is the hyperbolic space $\mathbb{H}^3$ using the upper half space model.

1.1 Constant Curvature Metrics

All surfaces admit constant Gauss curvature metrics. Surfaces with positive, zero and negative Euler numbers admit spherical, Euclidean and hyperbolic metrics respectively. Namely, all surfaces can have one of the three geometries, the spherical, Euclidean and hyperbolic geometry. Because most surfaces have negative Euler number, therefore, most surfaces have hyperbolic metrics. The canonical constant curvature metric plays an important role in geometric processing, especially for surface parameterizations.

This fact also holds for 3-manifolds. All 3-manifolds can be canonically decomposed to prime 3-manifolds. All prime 3-manifolds can be further decomposed by tori into pieces so that each piece has one of eight canonical geometries. Similar to the surface case, most 3-manifolds have hyperbolic metric, which induces constant sectional curvature. Finding the constant curvature metrics for 3-manifolds is an fundamental problem that is important for volumetric parameterization and analysis. This paper aims at introducing an algorithm to compute the constant curvature metric for hyperbolic 3-manifolds with boundaries.

(a)Left view

(b) Right view

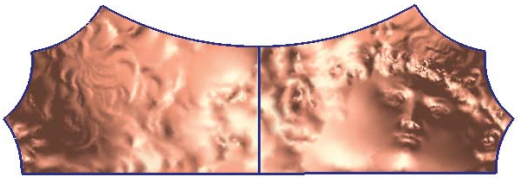

(c) Fundamental domain

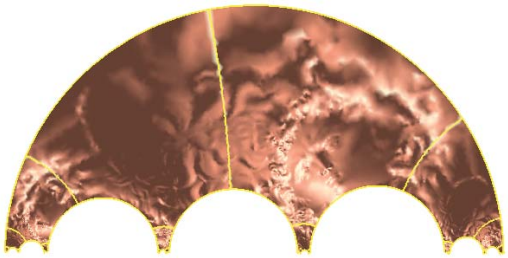

(d) Periodic embedding

Figure 1: Surface with boundaries with negative Euler number can be conformally periodically mapped to the hyperbolic space $\mathbb{H}^2$.

1.2 Discrete Curvature Flow

In order to compute the constant curvature metric of surfaces, the surfaces are approximated by triangular meshes. The metric is represented as the edge lengths. The Gaussian curvature is represented as discrete vertex curvature as shown in figure 8. Discrete curvature flow is an effective method to compute the metric on the meshes. The basic principle is to deform the edge lengths of the mesh according to the vertex curvatures, such that the curvature evolves according to a heat diffusion process. At the steady state, the metric is the constant curvature metric. Suppose the Euler number of the mesh is positive, zero or negative, we

treat each triangle on the mesh as a spherical, a Euclidean or a hyperbolic triangle. In the computation, we use spherical, Euclidean or hyperbolic cosine law.

The method can be generalized to 3-manifold directly. The 3-manifold is triangulated, and the edge lengths determine the metric. The edge lengths are deformed according to the curvature. At the steady state, the metric is the constant sectional curvature metric. In current work, we focus on hyperbolic 3-manifold only. During the computation, we assume all the tetrahedra are hyperbolic.

1.3 Differences between Surfaces and 3-Manifolds

There are fundamental differences between surfaces and 3-manifolds. The *Mostow rigidity* is the most prominent one [14]. Mostow rigidity states that the geometry of a finite volume hyperbolic manifold (for dimension greater than two) is determined by the fundamental group and hence unique. Namely, suppose M and N are complete finite volume hyperbolic n-manifolds with $n > 2$. If there exists an isomorphism $f : \pi_1(M) \to \pi_1(N)$ then it is induced by a unique isometry from M to N. For surface case, the geometry of the surface is not determined by the fundamental group. Suppose M and N are two surfaces with hyperbolic metrics. If M and N share the same topology, then there exist isomorphisms $f : \pi_1(M) \to \pi_1(N)$. But there may not exist an isometry from M to N. If we fix the fundamental group of the surface M, then there are infinite many pairwise non-isometric hyperbolic metrics on M. Each of them corresponding to a conformal structure of M.

Namely, surfaces have conformal geometry, 3-manifolds don't have conformal geometry. Suppose $\mathbf{g}_1$ and $\mathbf{g}_2$ are two Riemannian metrics on a topological surface S. If there is a function $\lambda : S \to \mathbb{R}$, such that $\mathbf{g}_1 = e^{2\lambda}\mathbf{g}_2$, then all the Riemannian metrics on the topological surface S can be classified by the conformal equivalence relation, each equivalence class is a *conformal structure*. If the surface is with a negative Euler number, then there exists a unique hyperbolic metric in each conformal structure. Given a surface embedded in $\mathbb{R}^3$, it has the induced Euclidean metric. The constant curvature metric obtained by curvature flow method is *conformal* to the original induced Euclidean metric.

Conformality is an important criteria for surface parameterization. Conformal surface parameterization is equivalent to find a metric with constant Gaussian curvature conformal to the induced Euclidean metric. For 3-manifold parameterizations, conformality can not be achieved in general. Surface parameterizations need the original induced Euclidean metric, namely, the vertex positions or the edge lengths are essential parts of the input. In contrast, for 3-manifolds, only

topological information is required. The tessellation of a surface will affect the conformality of the parameterization result. The tessellation doesn't affect the computational results of 3-manifolds. In order to reduce the computational complexity, we can use the simplest triangulation for a 3-manifold. For example, the 3-manifold of Thurston's Knotted Y-Shape in Fig.3 can be either represented as a high resolution tetrahedral mesh or a mesh with only 2 truncated tetrahedra, the resulting canonical metrics are identical. Meshes with very few tetrahedra are highly desired.

In practice, on discrete surfaces, there are only vertex curvatures, which measure the angle deficient at each vertex. On discrete 3-manifolds, like a tetrahedral mesh, there are both vertex curvatures and edge curvatures. The vertex curvature equals to 4π minus all the surrounding solid angles; the edge curvature equals to 2π minus all the surrounding dihedral angles. The vertex curvatures are determined by the edge curvatures. In our computational algorithm, we mainly use the edge curvature.

1.4 Contributions

This work generalizes discrete hyperbolic curvature flow from surface case to hyperbolic 3-manifold with geodesic boundaries and develop practical algorithms to compute the hyperbolic metrics of 3-manifolds. The algorithm is rigorous and efficient.

The rest of the paper is organized as follows: we briefly review the most related works in Section 2; details of the algorithms are explained in Section 3; Experimental results are reported in Section 4; We conclude in Section 5 with future directions.

2 Previous Works

Discrete surface curvature flow has been applied for surface parameterizations. Extensive research has been done on surface parameterization due to its wide applications in computer graphics. The surveys of [4, 17] provide excellent reviews on various kinds of mesh parameterization techniques. The followings methods in fact conformally deform the metrics and compute a metric with zero Gaussian curvature everywhere. Sheffer and Sturler introduced angle based flattening (ABF) method for surface parameterization in [15], the method was improved to be faster and more robust in [16]. A linear angle based parameterization method

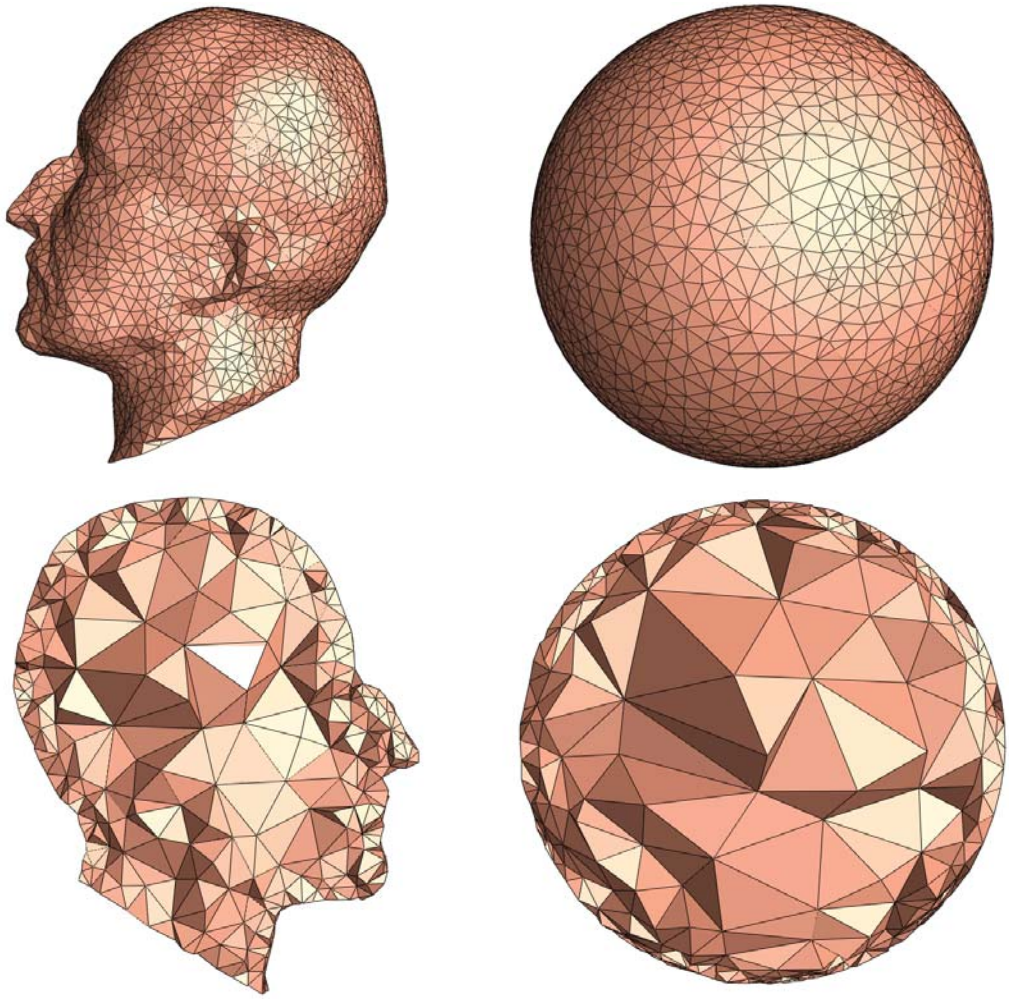

Figure 2: Volumetric parameterization for a topological ball.

is introduced in [22]. Circle pattern method for surface parameterization was introduced in [8]. Discrete Ricci flow method was applied for parameterizations of general surfaces in [7]. Ben-Chen et al. introduced a linear algorithm for designing metrics from curvatures in [3].

In the following, we briefly review some most related work on volumetric meshing and isosurface extraction. Labelle and Shewchuk introduced the isosurface stuffing algorithm to generate tetrahedron mesh with bounded dihedral angles in [10]. The volumetric discrete Laplace-Beltrami operator used in this work is a generalization of the cotan formula in the surface case; the cotan value of dihedral

angles are used to replace those of corner angles. The range of the dihedral angles affect the parameterization quality. A Delaunay-based variational approach to isotropic tetrahedral meshing is introduced by Alliez et al. in [1], which produces well-shaped tetrahedra by minimizing an energy form. Tandem algorithm is introduced for isosurfaces extraction and simplification in [2]. The volumetric harmonic map depends on volumetric Laplacian, volumetric graph Laplacian has been applied for large mesh deformation in [23].

Volumetric parameterization based on harmonic maps is applied for volumetric brain mapping in medical imaging field in [21]. In that work, the cotangent formula for discrete Laplace-Beltrami operator is generalized to tetrahedron mesh. Volumetric parameterization using fundamental solution method is introduced in [11] and applied for volumetric deformation and morphing. Harmonic volumetric paramaeterization for cylinder volumes is applied for constructing trivariate spline fitting in [13].

The topology and geometry of general 3-manifolds are explained in Thurston's works [19, 20]. Hyperbolic 3-manifolds with geodesic boundaries are manually constructed and analyzed in [6] and [5]. The theoretic foundation of our discrete curvature flow method is introduced in [12]. The topological method to verify whether a 3-manifold is hyperbolic manifold with complete geodesic boundaries is described in [19, 20].

3 Algorithm

The input to the algorithm is the boundary surface of a 3-manifold, represented as a triangular mesh. The output is a realization of (fundamental domain of) the 3-manifold in the hyperbolic space $\mathbb{H}^3$. The algorithm pipeline is as the following:

1. Compute the triangulation of the 3-manifold as a tetrahedral mesh. Simplify the triangulation such that the number of the tetrahedra is minimal.

2. Run discrete curvature flow on the minimal tetrahedral mesh.

3. Realize the minimal tetrahedral mesh in the hyperbolic space $\mathbb{H}^3$.

4. Real time display the 3-manifold with hyperbolic metric in $\mathbb{H}^3$ using image-based CSG rendering.

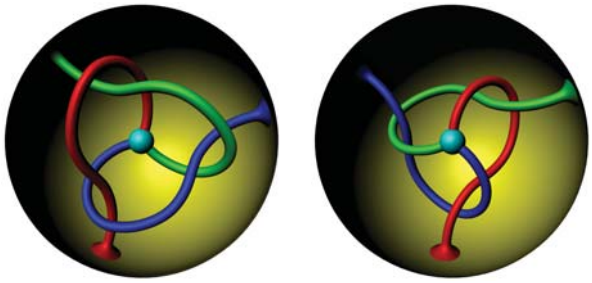

(a) Front view (b) Back view

Figure 3: The boundary surface of a 3-manifold, Thurston's knotted Y. The volume can be treated as a solid ball with three entangled pipes removed. Note that the spherical boundary surface is rendered using back-facing mode.

3.1 Triangulation and Simplification

In geometric processing, surfaces are approximated by triangular meshes. 3-manifolds are approximated by tetrahedral meshes. In general, given the boundary surfaces of a 3-manifold, there are existing methods to tessellate the interior and construct the tetrahedral mesh. In this work, we use tetrahedral tessellation based on volumetric Delaunay triangulation [18].

In order to simplify the triangulation, we use the following algorithm.

1. Denote the boundary of a 3-manifold M as $\partial M = \{S_1, S_2, \cdots, S_n\}$. For each boundary surface S_i, create a cone vertex v_i, connect each face $f_j \in S_i$ to form a tetrahedron T_j^i. Therefore, M is augmented to $\tilde{M}$.

2. Use *edge collapse* as shown in figure 5 to simplify the triangulation, such that all vertices are removed except for those cone vertices $\{v_1, v_2, \cdots, v_n\}$. Denote the simplified tetrahedral mesh still as $\tilde{M}$.

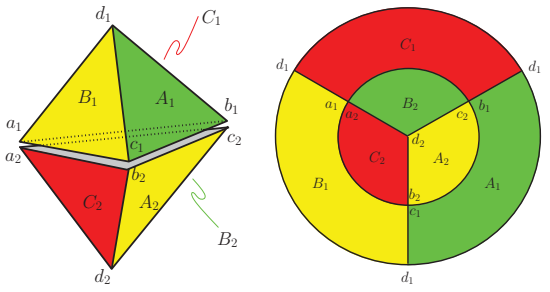

Figure 4: Simplified triangulation and gluing pattern of Thurston's knotted-Y. The two faces with the same color are glued together.

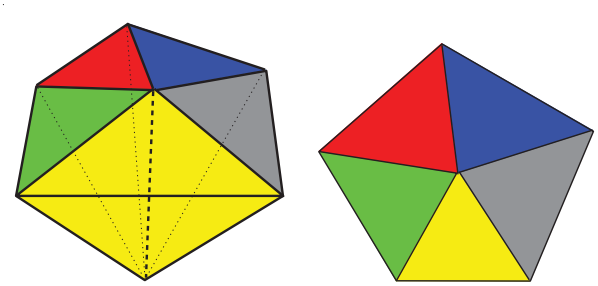

Figure 5: Edge collapse in tetrahedron mesh.

3. For each tetrahedron $\tilde{T}_i \in \tilde{M}$, cut $\tilde{T}$ by the boundary surfaces to form truncated tetrahedron (hyper ideal tetrahedron), denoted as T_i.

The simplified triangulation is represented as a collection of truncated tetrahedra and their gluing pattern. As shown in figure 4, the simplified tetrahedral mesh has only two truncated tetrahedra T_1, T_2. Let A_i, B_i, C_i, D_i represent the four faces of the tetrahedron T_i; a_i, b_i, c_i, d_i represent the truncated vertices of T_i. The gluing pattern is given as follows:

$$\begin{array}{ll} A_1 \to B_2 & \{b_1 \to c_2, d_1 \to a_2, c_1 \to d_2\} \\ B_1 \to A_2 & \{c_1 \to b_2, d_1 \to c_2, a_1 \to d_2\} \\ C_1 \to C_2 & \{a_1 \to a_2, d_1 \to b_2, b_1 \to d_2\} \\ D_1 \to D_2 & \{a_1 \to a_2, b_1 \to c_2, c_1 \to b_2\} \end{array}$$

The first row means that face $A_1 \in T_1$ is glued with $B_2 \in T_2$, such that the truncated vertex b_1 is glued with c_2, d_1 with a_2 and c_1 with d_2. Other rows can be interpreted in the same way.

3.2 Discrete Curvature Flow for 3-Manifolds

2-manifolds (surfaces) are approximated by triangular meshes with different background geometries. Similarly, 3-manifolds are approximated by tetrahedron meshes with different background geometry. 3-manifolds with boundaries can also be approximated by truncated tetrahedron meshes, where the face hexagons are glued together, the vertex triangles form the boundary surface.

3.2.1 Hyperbolic Cosine Law

As shown in figure 6, hyperbolic triangles and right angled hexagons satisfy special cosine laws.

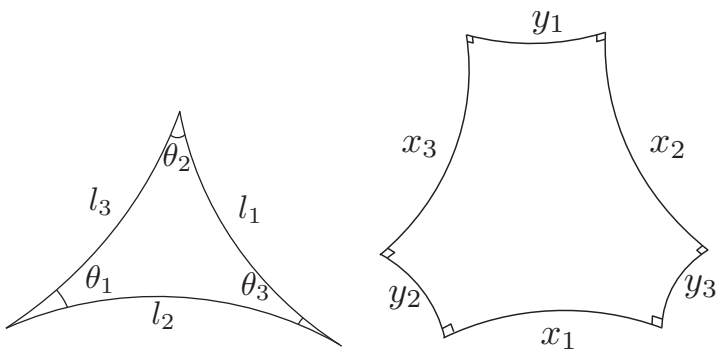

Figure 6: Hyperbolic Cosine laws for triangle and right-angled hexagon.

Given a triangle in the hyperbolic space $\mathbb{H}^2$, whose edge lengths are $\{l_i, l_j, l_k\}$ and the inner angles are $\{\theta_i, \theta_j, \theta_k\}$, where θ_i is against l_i, the inner angles are determined by the edge lengths according to the hyperbolic cosine law

$$\cosh l_i = \frac{\cos\theta_i + \cos\theta_j \cos\theta_k}{\sin\theta_j \sin\theta_k} \tag{3.1}$$

$$\cos\theta_i = \frac{-\cosh l_i + \cosh l_j \cosh l_k}{\sinh l_j \sinh l_k} \tag{3.2}$$

Given a hyperbolic hexagon as shown in figure 6 with all the right inner angles, the edge lengths are $\{x_i, x_j, x_k\}$, $\{y_i, y_j, y_k\}$, x_i is against y_i, then the cosine law for right-angled hyperbolic hexagon is

$$\cosh y_i = \frac{\cosh x_i + \cosh x_j \cosh x_k}{\sinh x_j \sinh x_k} \tag{3.3}$$

3.2.2 Hyperbolic Tetrahedron and Truncated Hyperbolic Tetrahedron

A closed 3-manifold can be triangulated to tetrahedra. The left frame in Figure 7 shows a hyperbolic tetrahedron $[v_1v_2v_3v_4]$. Each face f_i of a hyperbolic tetrahedron is a hyperbolic plane, each edge e_{ij} is a hyperbolic line segment. The right frame in Figure 7 shows a truncated hyperbolic tetrahedron, where the four vertices are truncated by hyperbolic planes. The cutting plane at vertex v_i is perpendicular to the edges e_{ij}, e_{ik}, e_{il}. Therefore, each face of a truncated hyperbolic tetrahedron is a right-angled hyperbolic hexagon, each cutting section is a hyperbolic triangle.

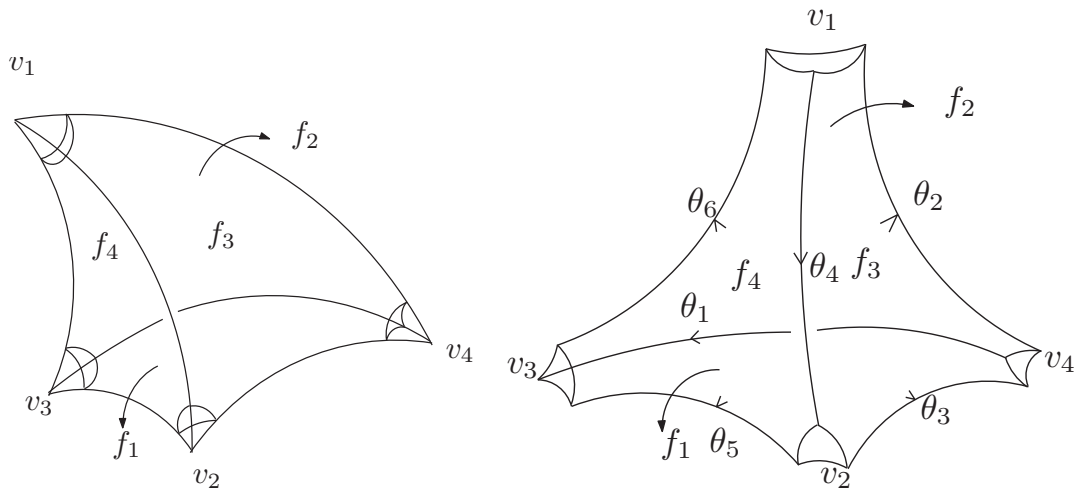

Figure 7: Hyperbolic tetrahedron and truncated tetrahedron.

As shown in Figure 7, the dihedral angles are $\{\theta_1, \theta_2, \cdots, \theta_6\}$. The geometry of the truncated tetrahedron is determined by these angles. For example, the hyperbolic triangle at v_2 has inner angles $\theta_3, \theta_4, \theta_5$, its edge lengths can be determined using formula 3.1. For face f_4, the edge length e_{12}, e_{23}, e_{31} are determined by the hyperbolic triangles at v_1, v_2, v_3 using the right-angled hyperbolic hexagon cosine law 3.3.

On the other hand, the geometry of a truncated tetrahedron is determined by the length of edges $e_{12}, e_{13}, e_{14}, e_{23}, e_{34}, e_{42}$. Due to the fact that each face is a right angled hexagon, the above six edge lengths will determine the edge lengths of each vertex triangle, and therefore determines its three inner angles, which equal to the corresponding dihedral angles.

3.2.3 Discrete Curvature

In the surface case, the discrete curvature is represented as the angle deficit. For an interior vertex, the curvature is 2π minus the surrounding corner angles;

$$K(v_i) = 2\pi - \sum_{jk} \alpha_i^{jk}.$$

for a boundary vertex, the curvature is π minus the surrounding corner angles. In 3-manifold case, as shown in figure 8, each tetrahedron $[v_i, v_j, v_k, v_l]$ has four solid angles at their vertices, $\{\alpha_i^{jkl}, \alpha_j^{kli}, \alpha_k^{lij}, \alpha_l^{ijk}\}$; for an interior vertex, the vertex

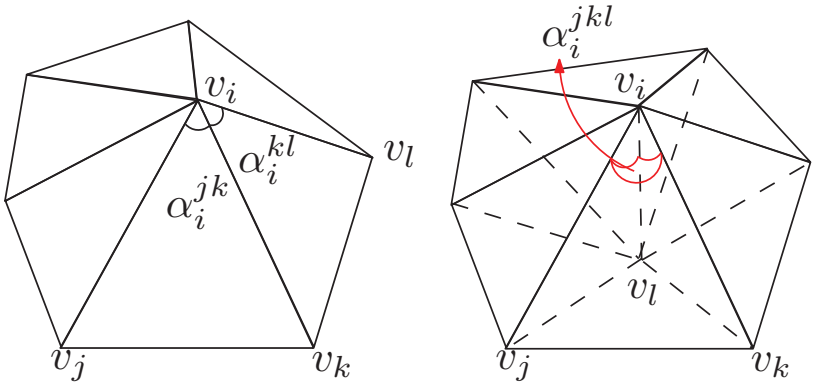

Figure 8: Discrete vertex curvature for 2-manifold and 3-manifold.

curvature is 4π minus the surrounding solid angles,

$$K(v_i) = 4\pi - \sum_{jkl} \alpha_i^{jkl}.$$

for a boundary vertex, the vertex curvature is 2π minus the surrounding solid angles.

In 3-manifold case, there is another type of curvature, *edge curvature*. Suppose $[v_i, v_j, v_k, v_l]$ is a tetrahedron, the dihedral angle on edge e_{ij} is denoted as β_{ij}^{kl}. If edge e_{ij} is an interior edge (i.e. e_{ij} is not on the boundary surface), its curvature is defined as

$$K(e_{ij}) = 2\pi - \sum_{kl} \beta_{ij}^{kl}.$$

If e_{ij} is on the boundary surface, its curvature is defined as

$$K(e_{ij}) = \pi - \sum_{kl} \beta_{ij}^{kl}.$$

For 3-manifolds, edge curvature is more essential than vertex curvature. The later is determined by the former.

Theorem Suppose M is a tetrahedron mesh, v_i is an interior vertex of M. Then

$$\sum_j K(e_{ij}) = K(v_i).$$

Proof: Draw a sphere centered at v_i, with a radius small enough such that the sphere only contains a single vertex v_i. The sphere intersects all the faces of the

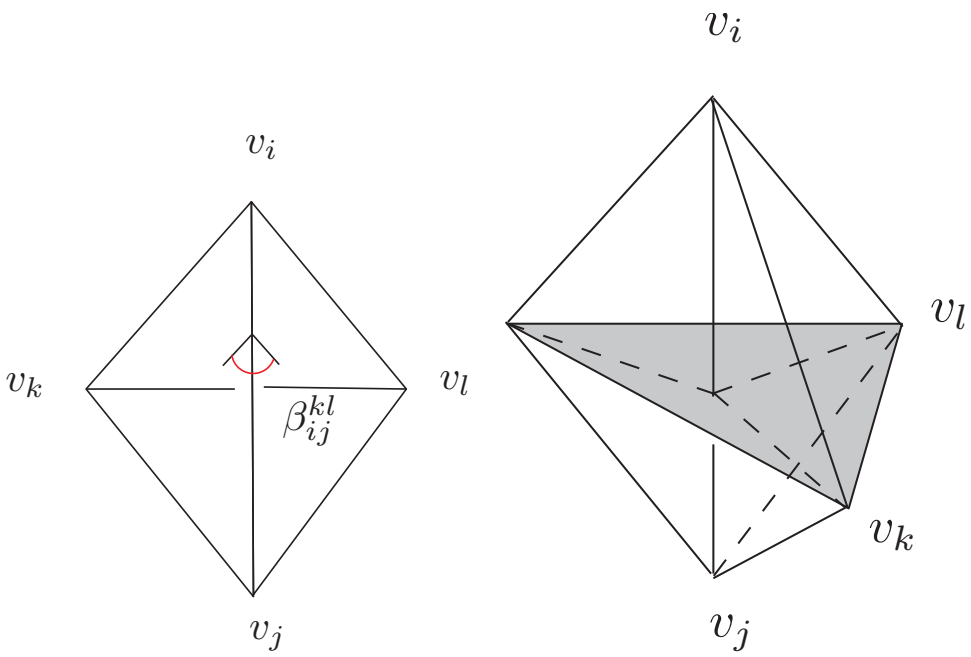

Figure 9: Discrete edge curvature for a 3-manifold.

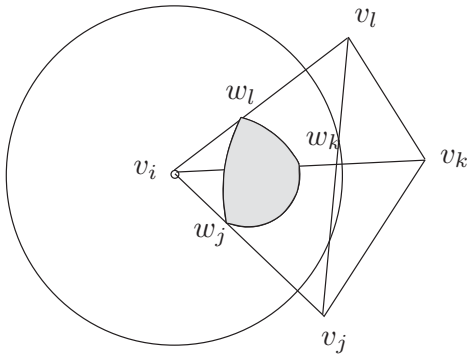

Figure 10: Vertex curvature and edge curvature are related.

mesh, which induces a triangulation of the sphere. Let $e_{ij} = [v_i, v_j]$ be an adjacent edge, e_{ij} intersects the sphere at w_j. Scale the sphere to be the unit sphere S. Now, each triangular face of S $[w_j, w_k, w_l]$ corresponds to the solid angle of an adjacent tetrahedron $[v_i, v_j, v_k, v_l]$; The discrete vertex curvature of S at w_j corresponds to the discrete edge curvature of edge e_{ij}. According to Gauss-Bonnet theorem, we

have

$$\sum_{jkl} A([w_j, w_k, w_l]) + \sum_j K(w_j) = 4\pi,$$

and therefore

$$\sum_j K(w_j) = \sum_j K(e_{ij} = 4\pi - \sum_{jkl} A([w_j, w_k, w_l]) = K(v_i).$$

3.2.4 Discrete Curvature Flow

Given a hyperbolic tetrahedron in $\mathbb{H}^3$ with edge lengths l_{ij} and dihedral angles θ_{ij}, the volume of the tetrahedron V is a function of the dihedral angles $V = V(\theta_{12}, \theta_{13}, \theta_{14}, \theta_{23}, \theta_{24}, \theta_{34})$, and the Schlaefli formula can be expressed as

$$\frac{\partial V}{\partial \theta_{ij}} = \frac{-l_{ij}}{2},$$

namely, the differential 1-form dV is $\frac{-1}{2}\sum_{ij} l_{ij} d\theta_{ij}$. It can be further proved that the volume of a hyperbolic truncated tetrahedron is a strictly concave function of the dihedral angles.

Given an ideal triangulated 3-manifold (M, T), let E be the set of edges in the triangulation. An assignment $x : E \to \mathbb{R}^+$ is called a *hyperbolic cone metric associated with the triangulation* T if for each tetrahedron t in T with edges $e_1, e_2, \cdots, e_6$, the $x(e_i)$ are the edge lengths of a hyperbolic truncated tetrahedron in $\mathbb{H}^3$. The set of all hyperbolic cone metrics associated with T is denoted as $L(M, T)$, which is an open set. The discrete curvature of a cone metric is a map $K(x) : L \to R$, mapping each edge e to its discrete curvature. The discrete curvature flow is then defined by

$$\frac{dx_{ij}}{dt} = K_{ij}, \tag{3.4}$$

where x_{ij} is the edge length of e_{ij}, K_{ij} is the edge curvature of e_{ij}.

For any ideal triangulated 3-manifold (M, T), the equilibrium points of the discrete curvature flow Eqn.3.4 are the complete hyperbolic metric with totally geodesic boundary. Each equilibrium is a local attractor of the flow. Furthermore, a hyperbolic cone metric associated with an ideal triangulation is locally determined by its cone angles. For any ideal triangulated 3-manifold, under the discrete curvature flow, the discrete curvature $K_{ij}(t)$ evolves according to the discrete heat equation. Furthermore, the total curvature $\sum_{ij} K_{ij}^2$ is strictly decreasing until all edge curvatures (also the vertex curvatures) are zeros. The theoretic proofs can be found in [12].

3.3 Hyperbolic Embedding of 3-Manifolds

Once the edge lengths of the tetrahedron mesh have been obtained, we can realize it in the hyperbolic space $\mathbb{H}^3$. First, we introduce how to construct a single truncated tetrahedron; then we explain how to glue multiple truncated tetrahedra by hyperbolic rigid motion.

3.3.1 Hyperbolic Space Model

In this work, we use the upper half plane model for hyperbolic space $\mathbb{H}^2$. $\mathbb{H}^2 = \{(x, y) \in \mathbb{R}^2 | y > 0\}$, with the Riemannian metric $ds^2 = \frac{dx^2+dy^2}{y^2}$. In $\mathbb{H}^2$, hyperbolic lines are circular arcs and half lines orthogonal to the x-axis. The rigid motion is given by the so-called *Möbius transformation*

$$\frac{az + b}{cz + d}, ac - bd = 1, a, b, c, d \in \mathbb{R},$$

where $z = x + iy$ is the complex coordinates.

Similarly, the three dimensional hyperbolic space $\mathbb{H}^3$ can be represented using upper half space model,$\mathbb{H}^3 = \{(x, y, z) \in \mathbb{R}^3 | z > 0\}$, with Riemannian metric

$$ds^2 = \frac{dx^2 + dy^2 + dz^2}{z^2}.$$

In $\mathbb{H}^3$, the hyperbolic planes are hemispheres or vertical planes, whose equators are on the xy-plane. The xy-plane represents all the infinity points in $\mathbb{H}^3$. The rigid motion in H^3 is determined by its restriction on the xy-plane, which is a Möbius transformation on the plane, in the form

$$\frac{az + b}{cz + d}, ac - bd = 1, a, b, c, d \in \mathbb{C}.$$

Most of the computation is carried out on the xy-plane.

3.3.2 Construction of a Truncated Hyperbolic Tetrahedron

The geometry of a truncated hyperbolic tetrahedron is determined by its dihedral angles. This section explains the algorithm to construct a truncated tetrahedron in the upper half space model of $\mathbb{H}^3$. The algorithm consists of two steps. First, construct a circle packing; second, compute a CSG (Constructive Solid Geometry) surface. The resulting surface is the boundary of the truncated tetrahedron.

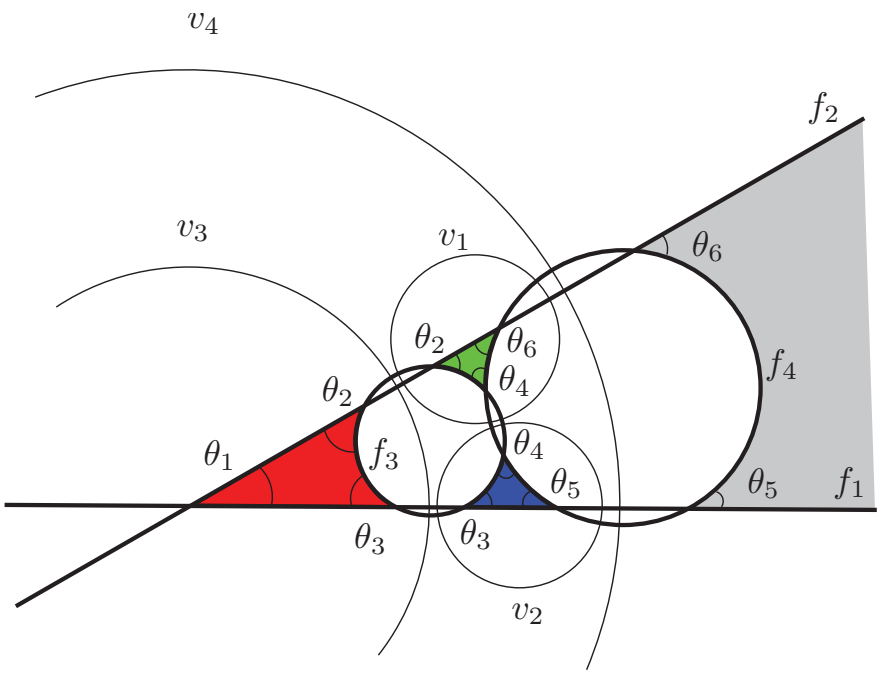

Figure 11: Circle packing for the truncated tetrahedron.

Construct a Circle Packing Suppose the dihedral angles of a truncated tetrahedron are given. The tetrahedron can be realized in $\mathbb{H}^3$ uniquely, up to rigid motion. The tetrahedron is the intersection of half spaces, the boundaries of these half spaces are the hyper planes on faces f_1, f_2, f_3, f_4 and the cutting planes at the vertices v_1, v_2, v_3, v_4. Each plane intersects the infinity plane at a hyperbolic line, which is a Euclidean circle on the xy-plane. By abusing the symbols, we use f_i to represent the intersection circle between the hyperbolic plane through the face f_i and the infinity plane. Similarly, we use v_j to represent the intersection circle between the cutting plane at v_j and the infinity plane. The goal of this step is to find planar circles f_i's and v_j's, such that

1. circle f_i and circle f_j intersect at the given corresponding angle.
2. circle v_i is orthogonal to circles f_j, f_k, f_l.

As shown in figure 11, all the circles can be computed explicitly.

- f_1, line $y = 0$.
- f_2, line $y = \tan\theta_1 x$.

- f_3, circle with radius 1, and centered at

$$(x_3, y_3) = (\frac{\cos\theta_1 \cos\theta_3 + \cos\theta_2}{\sin\theta_1}, \cos\theta_3)$$

- f_4, circle with radius

$$R = \frac{\sqrt{(\cos\theta_4 + a + b)^2 - c(1 - x_3^2 - y_3^2)} - (\cos\theta_4 + a + b)}{c},$$

where

$$(a, b, c) = (\cos\theta_5, \frac{\cos\theta_5 \cos\theta_1 + \cos\theta_6}{\sin\theta_1}, 1 - a^2 - b^2)$$

and centered at (aR, bR).

In order to compute the circles v_i's, we use the fact that v_i is orthogonal to circles f_j, f_k, f_l, where $\{i, j, k, l\}$ are pairwisely different. First we need to transform f_1 and f_2 from lines to Euclidean circles. Let p, q be two points, which are not on any circle f_j, define a Möbius transformation

$$\phi = \frac{z - q}{z - p}, \phi^{-1} = \frac{pw - q}{w - 1}.$$

Then ϕ^{-1} transforms f_1, f_2, f_3, f_4 to circles, and circle v_1 is orthogonal to circle f_2, f_3, f_4, as shown 12. Such a circle exists and is unique; it can be computed explicitly by solving the following system,

$$(x_1 - x_j)^2 + (y_1 - y_j)^2 = r_j^2 + r_1^2, j = 2, 3, 4$$

where (x_1, y_1) is the center, r_1 is the radius of v_1. After finding v_1, v_2, v_3, v_4, we transform them back using ϕ. Let w_1, w_2, w_3 be points on the circle v_1, the $\phi(w_1), \phi(w_2), \phi(w_3)$ are the points on the circle $\phi(v_1)$.

CSG Modeling After we obtain the circle packing, we can construct hemispheres whose equators are those circles. If the circle is a line, then we construct a half plane orthogonal to the xy-plane through the line. Computing CSG among these hemispheres and half-planes, we can get the truncated tetrahedron as shown in figure 13.

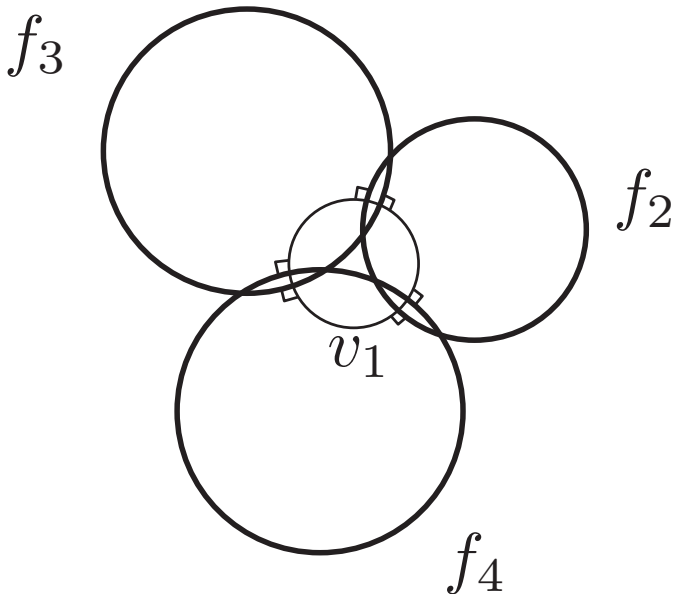

Figure 12: Circle v_1 is orthogonal to circles f_2, f_3, f_4.

Each hemisphere is a hyperbolic plane, and separates $\mathbb{H}^3$ to two half-spaces. For each hyperbolic plane, we select one half-space; the intersection of all such half-spaces is the desired truncated tetrahedron embedded in $\mathbb{H}^3$. The question is, we need to determine which half-space of the two is to be used. The answer is as the following. Here we use f_i to represent both the face circle and the hemisphere whose equator is the face circle f_i. Similarly, we use v_k to represent both the vertex circle and the hemisphere whose equator is the vertex circle. As shown in figure 11, three face circles f_i, f_j, f_k bound a curved triangle Δ_{ijk}, which is color coded, one of them is infinite. If Δ_{ijk} is inside the circle f_i, then we choose the half space inside the hemisphere f_i; otherwise we choose the half-space outside the hemisphere f_i. Suppose vertex circle v_k is orthogonal to the face circles f_i, f_j, f_k; if Δ_{ijk} is inside the circle v_k, then we choose the half-space inside the hemisphere v_k; otherwise we choose the half-space outside the hemisphere v_k.

Figure 14 demonstrates a realization of a truncated hyperbolic tetrahedron in the upper half space model of $\mathbb{H}^3$, based on the circle packing in figure 11.

3.3.3 Glue two Truncated Hyperbolic Tetrahedra

Suppose we want to glue two truncated hyperbolic tetrahedra, T_1 and T_2, along their faces. We need to specify the correspondence between the vertices and faces

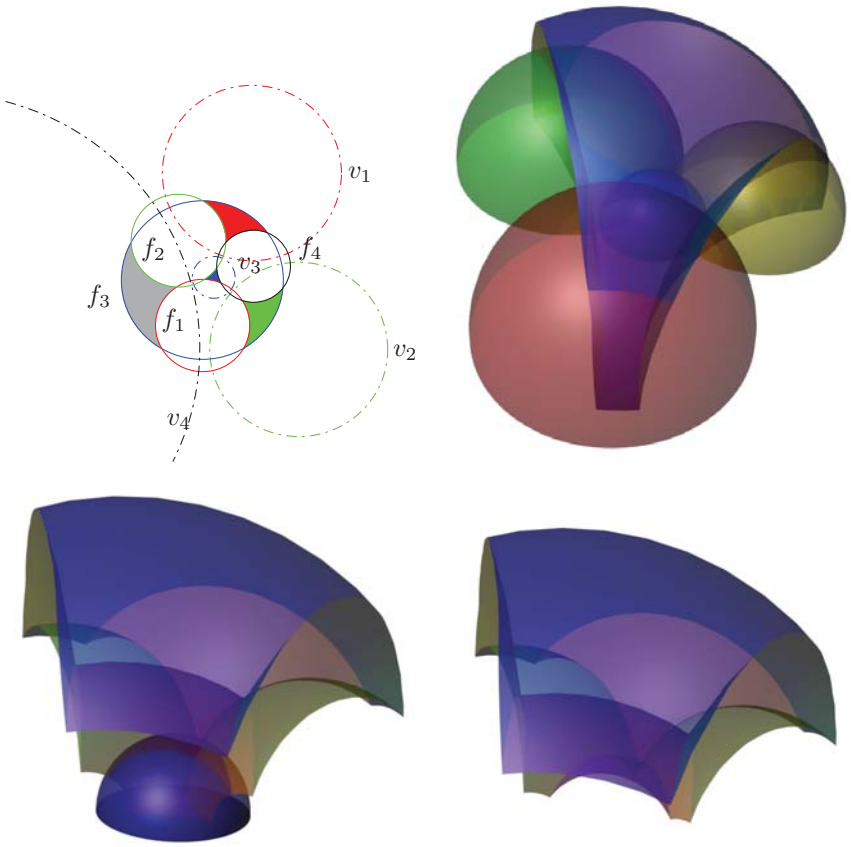

Figure 13: Constructing an ideal hyperbolic tetrahedron from circle packing using CSG operators.

between T_1 and T_2. Suppose we want to glue $f_4 \in T_1$ to $f_l \in T_2$, such that $\{v_1, v_2, v_3\} \subset T_1$ are attached to $\{v_i, v_j, v_k\} \subset T_2$. Such a gluing pattern can be denoted as a permutation $\{1, 2, 3, 4\} \rightarrow \{i, j, k, l\}$. The right-angled hyperbolic hexagon of f_4 is congruent to the hexagon of f_l. Suppose the circle packing of f_4 is as shown in the last frame of figure 16, the intersection points between f_4 and v_3 are p and q, the intersection points between f_4 and v_1 are r and s; p, r, s, q are sorted counter-clockwisely along the circle of f_4. Then we construct a Möbius transformation

$$\phi_1(z) = \frac{(z-p)(r-q)}{(z-q)(r-p)},$$

Figure 14: Realization of a truncated hyperbolic tetrahedron in the upper half space model of $\mathbb{H}^3$, based on the circle packing in figure 11.

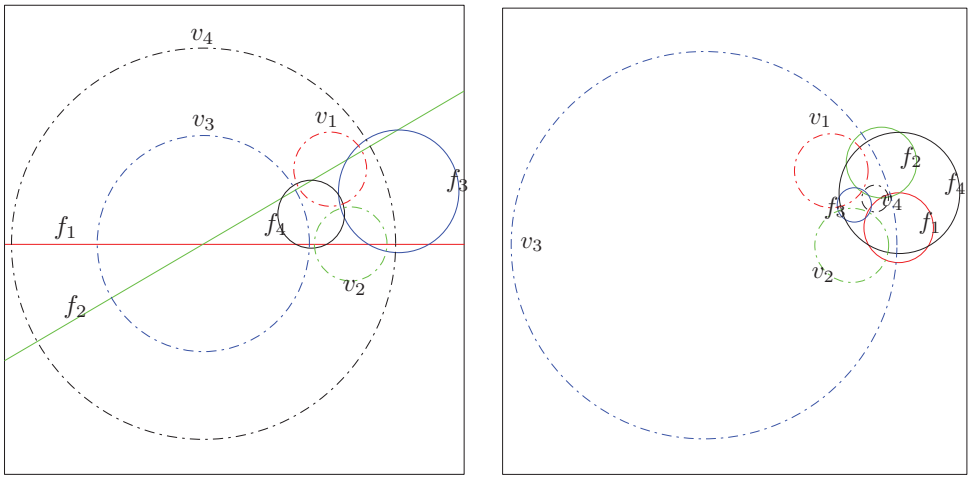

Figure 15: Glue two tetrahedra by using a Möbius transformation to glue their circle packings, such that $f_3 \to f_4$, $v_1 \to v_1, v_2 \to v_2, v_4 \to v_3$.

which maps p, r, q to $0, 1, \infty$. Similarly, suppose circle f_l intersects v_k at $\tilde{p}, \tilde{q}$, f_l intersects v_i at $\tilde{r}, \tilde{s}$, let

$$\phi_2(z) = \frac{(z-\tilde{p})(\tilde{r}-\tilde{q})}{(z-\tilde{q})(\tilde{r}-\tilde{p})},$$

then the Möbius transformation $\phi = \phi_2^{-1} \circ \phi_1$ induces an hyperbolic isometry that glues f_4 to f_l, $\{v_1, v_2, v_3\}$ to $\{v_i, v_j, v_k\}$.

Figure 17 shows the gluing between two truncated hyperbolic tetrahedra.

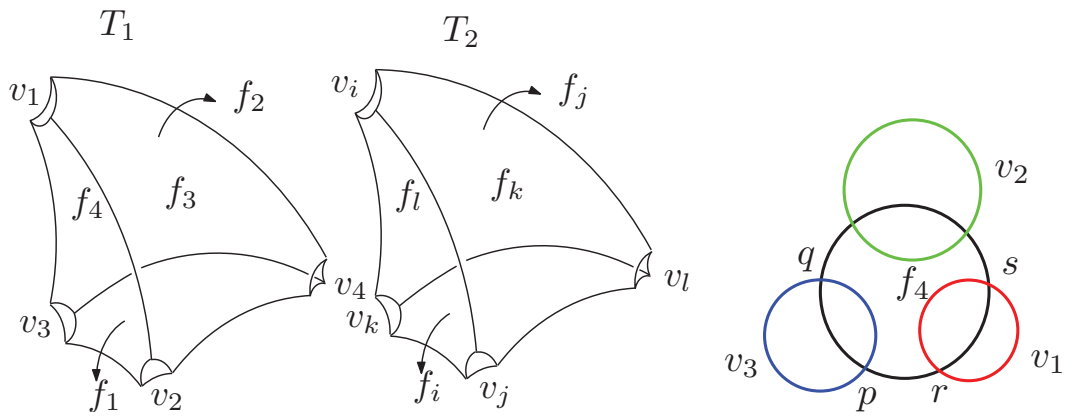

Figure 16: Glue T_1 and T_2 along $f_4 \in T_1$ and $f_l \in T_2$, such that $\{v_1, v_2, v_3\} \subset T_1$ are attached to $\{v_i, v_j, v_k\} \subset T_2$.

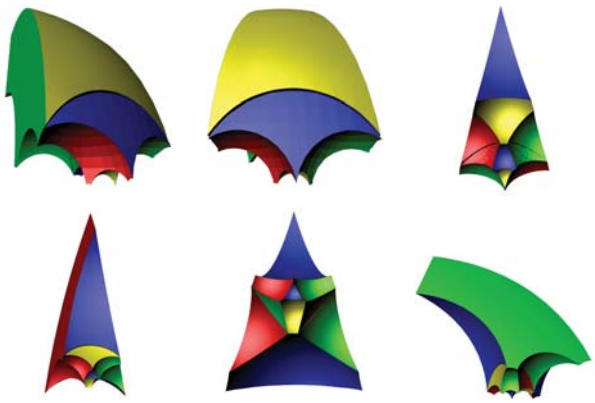

Figure 17: Glue T_1 and T_2. The first row, $f_3 \rightarrow f_4$, $\{v_1, v_2, v_4\} \rightarrow \{v_1, v_2, v_3\}$. The second row, $f_4 \rightarrow f_3$,$\{v_1, v_2, v_3\} \rightarrow \{v_2, v_1, v_4\}$.

The first row shows the change of the circle packing (only the face circles are illustrated, the vertex circles are omitted); the second row shows the different views of the transformed tetrahedron corresponding to the second circle packing in the first row; the third row shows the different views of the transformed tetrahedron corresponding to the last circle packing in the first row. 11.

3.4 Real Time Rendering

The periodic embedding of the 3-manifold in the hyperbolic space $\mathbb{H}^3$ can be rendered in real time using image-based CSG rendering technique [9]. More rigorously speaking, we can display the embedding of a finite portion of the universal covering space of M with the hyperbolic metric in $\mathbb{H}^3$ in real time.

The edge lengths and dihedral angles are pre-computed. The circle packing for each truncated tetrahedron is also precomputed. The gluing pattern and the CSG tree are generated on the fly. We use OpenCSG library to display the embedding in real time.

4 Experimental Results

Figure 18: Embed the 3-manifold periodically in the hyperbolic space $\mathbb{H}^3$.

We tested our algorithm extensively on more than 120 hyperbolic 3-manifolds tessellated by truncated hyperbolic tetrahedra. All the testing cases are convergent. We compare our computational results with those using algebraic geometry methods, the metrics and dihedral angles are perfectly matched. The matching error is less than $1e-8$.

The stability of the algorithm depends on several key factors:

- The choice of the triangulation. For the same 3-manifold, different triangulations affect the stability of the curvature flow. For some triangulation, the critical point of the volume energy is an interior point of the metric space. In this case, the discrete curvature flow is convergent and stable. For some triangulation, the critical point of the volume energy is on the boundary of

the metric space, the algorithm can not lead to the desired result. It is an open problem to find the conditions for the triangulations, which guarantee the convergence of the curvature flow.

- The choice of the initial conditions. Due to the numerical error, if the initial edge lengths are too big (greater than 37.7) then the angles computed using hyperbolic cosine law is too close to zeros. This leads to the instability. In practice, we choose the initial edge lengths around 1.0, which always gives the desired solutions.

We apply our discrete hyperbolic curvature flow to visualizing 3-manifolds, which can not be realized in $\mathbb{R}^3$ and given by abstract tetrahedron meshes. We also apply it to verifying whether two 3-manifolds are homeomorphic by comparing their hyperbolic volumes. If two hyperbolic 3-manifolds with geodesic boundaries are homeomorphic, then their hyperbolic volumes should be identical, independent of their triangulations.

5 Conclusion and Future Direction

This paper generalizes discrete curvature flow for surfaces to hyperbolic 3-manifolds with complete geodesic boundaries. The metric deforms according to the curvature, until the curvature is constant everywhere. The theoretical results are introduced, and the algorithm is explained in details. Thorough experimental results demonstrate the effectiveness and the efficiency of the 3-manifold curvature flow algorithm. The method is applied for visualizing 3-manifolds and volumetric shape analysis.

In the future, we will generalize the current method for computing geometric structures of 3-manifolds with other topological types. We will also study the conditions for triangulations to ensure the existence of the solutions. For real applications, we will apply discrete curvature flow method for parameterizing volumes in the three dimensional Euclidean space.

References

[1] Pierre Alliez, David Cohen-Steiner, Mariette Yvinec, and Mathieu Desbrun. Variational tetrahedral meshing. *ACM Trans. Graph.*, 24(3):617–625, 2005.

[2] Dominique Attali, David Cohen-Steiner, and Herbert Edelsbrunner. Extraction and simplification of iso-surfaces in tandem. In *Symposium on Geometry Processing*, pages 139–148, 2005.

[3] Mirela Ben-Chen, Craig Gotsman, and Guy Bunin. Conformal flattening by curvature prescription and metric scaling. *Computer Graphics Forum (Proc. Eurographics)*, 27(2), 2008.

[4] Michael S. Floater and Kai Hormann. Surface parameterization: a tutorial and survey. In *Advances in Multiresolution for Geometric Modelling*, pages 157–186. Springer, 2005.

[5] Roberto Frigerio, Bruno Martelli, and Carlo Petronio. Small hyperbolic 3-manifolds with geodesic boundary. *Experimental Mathematics*, 13:171–184, 2004.

[6] Michihiko Fujii. Hyperbolic 3-manifolds with totally geodesic boundary. *Osaka Journal of Mathematics*, 27:539–553, 1990.

[7] Miao Jin, Junho Kim, Feng Luo, and Xianfeng Gu. Discrete surface ricci flow. *IEEE Transaction on Visualization and Computer Graphics*, 2008.

[8] Liliya Kharevych, Boris Springborn, and Peter Schröder. Discrete conformal mappings via circle patterns. *ACM Transactions on Graphics*, 25(2):412–438, 2006.

[9] Florian Kirsch and Jürgen Döllner. Rendering techniques for hardware-accelerated image-based csg. In *WSCG*, pages 221–228, 2004.

[10] François Labelle and Jonathan Richard Shewchuk. Isosurface stuffing: fast tetrahedral meshes with good dihedral angles. *ACM Trans. Graph.*, 26(3):57, 2007.

[11] Xin Li, Xiaohu Guo, Hongyu Wang, Ying He, Xianfeng Gu, and Hong Qin. Harmonic volumetric mapping for solid modeling applications. In *Proceeding of Symposium on Solid and Physical Modeling*, pages 109–120, 2007.

[12] Feng Luo. A combinatorial curvature flow for compact 3-manifolds with boundary. *Electron. Res. Announc. Amer. Math. Soc.*, 11:12–20, 2005.

[13] Tobias Martin, Elaine Cohen, and Mike Kirby. Volumetric parameterization and trivariate b-spline fitting using harmonic functions. In *Proceeding of Symposium on Solid and Physical Modeling*, 2008.

[14] G. D. Mostow. Quasi-conformal mappings in n-space and the rigidity of the hyperbolic space forms. *Publ.Math.IHES*, 34:53–104, 1968.

[15] Alla Sheffer and Eric de Sturler. Parameterization of faced surfaces for meshing using angle based flattening. *Engineering with Computers*, 17(3):326–337, 2001.

[16] Alla Sheffer, Bruno Lévy, Maxim Mogilnitsky, and Alexander Bogomyakov. ABF++: Fast and robust angle based flattening. *ACM Transactions on Graphics*, 24(2):311–330, 2005.

[17] Alla Sheffer, Emil Praun, and Kenneth Rose. Mesh parameterization methods and their applications. *Foundations and Trends® in Computer Graphics and Vision*, 2(2), 2006.

[18] Hang Si. Tetgen: A quality tetrahedral mesh generator and three-dimensional delaunay triangulator. http://tetgen.berlios.de/.

[19] William Thurston. *The geometry and topology of 3-manifolds*. Princeton lecture notes, 1978-1981.

[20] William P. Thurston. Three-dimensional manifolds, kleinian groups and hyperbolic geometry. *Bull. Amer. Math. Soc. (N.S.)*, 6(3):357–381, 1982.

[21] Yalin Wang, Xianfeng Gu, Paul M. Thompson, and Shing-Tung Yau. 3d harmonic mapping and tetrahedral meshing of brain imaging data. In *Proceeding of Medical Imaging Computing and Computer Assisted Intervention (MICCAI), St. Malo, France*, 2004.

[22] Rhaleb Zayer, Bruno Lévy, and Hans-Peter Seidel. Linear angle based parameterization. In *Symposium on Geometry Processing*, pages 135–141, 2007.

[23] Kun Zhou, Jin Huang, John Snyder, Xinguo Liu, Hujun Bao, Baining Guo, and Heung-Yeung Shum. Large mesh deformation using the volumetric graph laplacian. *ACM Trans. Graph.*, 24(3):496–503, 2005.